JOURNAL OF PROPULSION AND POWER
Vol. 11, No. 2, March–April 1995

Photovoltaic Catenary-Tent Array for the Martian Surface

M. Crutchik*
Tel-Aviv University, Tel-Aviv 69978, Israel
Anthony J. Colozza†
Sverdrup Technology, Inc., Brook Park, Ohio 44135
and
J. Appelbaum‡
NASA Lewis Research Center, Cleveland, Ohio 44135

To provide electrical power during an exploration mission to Mars, a deployable tent-shaped structure with a flexible photovoltaic (PV) blanket is analyzed. The array is designed with a self-deploying mechanism utilizing pressurized gas expansion. The structural design for the array uses a combination of cables, beam, and columns to support and deploy the PV blanket. Under the force of gravity a cable carrying a uniform load will take the shape of a catenary curve. A catenary-tent collector is self-shadowing, which must be taken into account in the solar radiation calculation. The shape and the area of the shadow on the array has been calculated and used in the determination of the global radiation on the array. The PV blanket shape and structure dimensions were optimized to achieve a configuration that maximizes the specific power (W/kg). The optimization was performed for four types of PV blankets (Si, GaAs/Ge, GaAs CLEFT, and amorphous Si), and four types of structural materials (carbon composite, aramid fiber composite, aluminum and magnesium). The combination of carbon composite structural material and GaAs CLEFT solar cells produce the highest specific power. The study was carried out for two sites on Mars corresponding to the Viking lander locations. The designs were also compared for summer, winter, and yearly operation.

Introduction

THE ability to establish an outpost on the Martian surface is initially dependent on the availability of an adequate power source. The ideal power supply would require very little implementation time and have a high reliability for operation. Also, to meet the constraints of launching and transportation it would need to be lightweight and capable of being stowed in relatively small volume. A photovoltaic (PV) array whose configuration is optimized for maximum specific power (W/kg) can meet these requirements.

One structurally-efficient design for a nontracking solar array is the "tent" configuration that has been analyzed for solar arrays for the moon.[1-3] An advantage of the tent configuration is that it provides significant power shortly after the sun rises above the horizon, where a horizontal array has very low power at dawn and dusk due to low sun angles. The main advantage of a tent array over a tracking array is the increase in reliability due to the absence of moving parts that are subject to failure due to cold, wind, or thermal cycling. Most of the structural and operational advantages that make the tent design desirable for the moon are also applicable to Mars. On Mars it is also desirable to use an array that is lifted off the ground, and thus, less subject to dust deposition.

Structure Analyses

A tent-shaped structure with a flexible PV blanket for solar power generation was analyzed in Ref. 3. An artist's conception of the array is shown in Fig. 1. The array structure was designed to be capable of supporting a PV blanket and have the ability for autonomous deployment and compact stowage. In the stowed configuration the PV blanket is either folded or rolled, depending upon the particular blanket's flexibility. Upon deployment, the PV blanket is held in place on the structure by a series of cables that are evenly spaced along the blanket length. Under the force of gravity these cables, which are supporting the weight of the PV blanket, will take the shape of a catenary curve that is shown in Fig. 2 and given by

$$z = f_c(y)$$

$$f_c(y) = K(\cos h\{[(d/2 - y)/K] - 1\})$$

where K is the catenary constant determined by $f_c(0) = H$. The beams on which the cables are attached are supported by a series of telescoping columns which, by the use of a

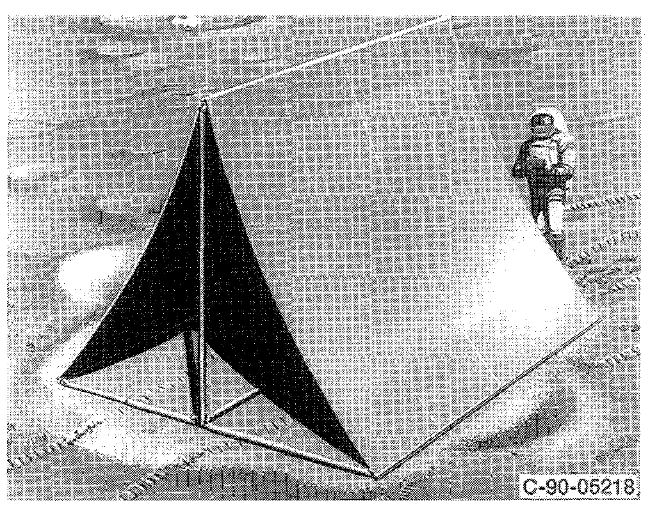

Fig. 1 Artists conception of a self-deploying PV tent array.

Received Aug. 21, 1993; revision received Feb. 7, 1994; accepted for publication Aug. 25, 1994.

*Research Assistant, Faculty of Engineering.

†Design Engineer, NASA Lewis Research Center Group. Member AIAA.

‡National Research Council—NASA Research Associate, Faculty of Engineering; currently Professor, Tel-Aviv University, Tel-Aviv 69978, Israel.

Table 1 PV blanket and structural materials specification

	a) Structural materials properties			
	Carbon VHS composite	Aramid fiber composite	Aluminum	Magnesium
Modulus, GPA	124	76	72	45
Yields strength, GPA	1.90	1.38	0.41	0.28
Density, kg/m^3	1530	1380	2800	1800
	b) PV blanket specifications			
	Silicon	GaAs/Ge	GaAs CLEFT	Amorphous silicon
Efficiency, %	14.5	19.5	20.0	10.0
Blanket specific, mass, kg/m^2	0.427	0.640	0.361	0.040
Cell thickness, μm	250	~250	20	2

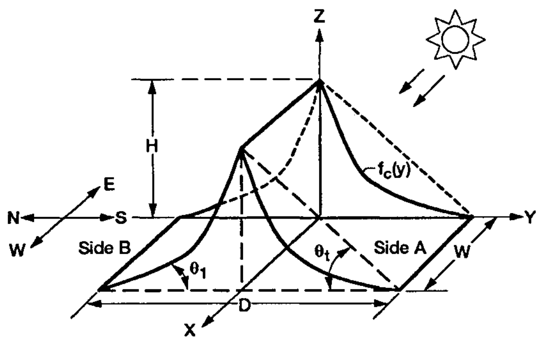

Fig. 2 Tent structure and PV blanket geometry.

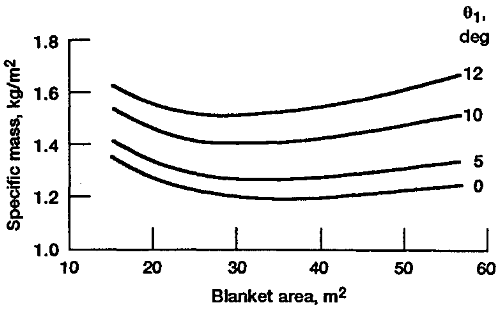

Fig. 3 Variation of the yearly average irradiance as function of tent azimuth angle.

pressurized gas system, also act as the deployment mechanism for the array.[3]

The structural analysis takes into account the tension in the blanket and support cables, weight of the structural components and PV blanket, forces incurred during deployment, and wind loading. The maximum loading on each structural component was determined based on the forces it would encounter during deployment and operation. The necessary dimensions of each component was then calculated based on the estimated loadings. The wind loadings were calculated for a worst-case situation in which the direction of the wind was 15 deg off the central axis of the array at a wind speed of 20 m/s.[3,4] In this situation the array would generate a maximum amount of lift and, therefore, force on the structure. The wind speed of 20 m/s was chosen as the design wind speed since 99.9% of the winds experienced on Mars by the Viking landers were below 20 m/s.[5] It should be noted that on Earth, wind loading constitutes the main loading force. On Mars, however, the wind loading is not nearly as great due to substantially lower atmospheric density, viz., about 7–9 mbar.

The structure design parameters, shown in Fig. 2, are the tent base length D, the tent width W, the tent height H, the tent angle θ_t, which is the angle that the blanket would make with the horizontal if it were pulled perfectly taut, and the blanket end angle θ_1, which is the actual angle the blanket makes with the horizontal at the base. The parameters given above, which designate the size and shape of the PV blanket, are determined by an optimization between minimizing structure mass and maximizing output power. The details of the structural analysis used to determine the component weights and dimensions are given in Ref. 3. This reference shows that the optimal blanket shape, which is characterized by the end angle θ_1 for minimum structure specific mass, is obtained for $\theta_1 = 0$, i.e., a blanket having a natural catenary shape. This result is shown in Fig. 3 for carbon very high strength (VHS) composite material, GaAs/Ge PV blanket, $\theta_t = 15$ deg and 20 m/s wind speed. Similar trends were obtained with all other material/PV blanket combinations.

The analysis was performed with four types of structural materials (carbon VHS composite, aramid fiber composite, aluminum, and magnesium), and with four types of PV blankets (silicon, gallium arsenide on germanium, gallium arsenide CLEFT and amorphous silicon). The properties of the structural materials and the PV blankets are given in Tables 1a[6,7] and 1b,[8,9] respectively. It should be noted that it was assumed that the composite material properties were isotropic, i.e., the composite materials were not optimized to resist loading along a particular direction.

Solar Power Analysis

A catenary-tent-collector is self-shadowing (e.g., side B is shadowed by side A in Fig. 2); this must be taken into account in determining the PV blanket output power. A detailed analysis of the shape and the area of the shadow on the array and, hence, the beam irradiance incident on the blanket, is given in Ref. 10. The diffuse and albedo irradiance were also calculated to determine the global irradiance on the array. A solar radiation model for Mars was developed in Ref. 11 and the solar output power of the PV blanket was determined based on this model.

There will be some shadowing of the array during the day due to the catenary tent-shaped configuration. This nonuniform illumination can lead to efficiency losses and hot-spot heating on the PV blanket affecting series connected cells. This analysis has assumed that the efficiency is independent of the shadow pattern.

The effect of the azimuthal orientation of the catenary tent on the irradiance was investigated and the results are shown in Fig. 4 for yearly average irradiance at Viking lander 1 (VL1) based on the solar radiation model. The figure shows the variation of the direct "beam" irradiance on both sides A and B of the PV blanket and the corresponding beam irradiance average. The diffuse irradiance is assumed to be independent of the azimuth, therefore, the global irradiance on the tent-blanket follows the variation of the beam. The

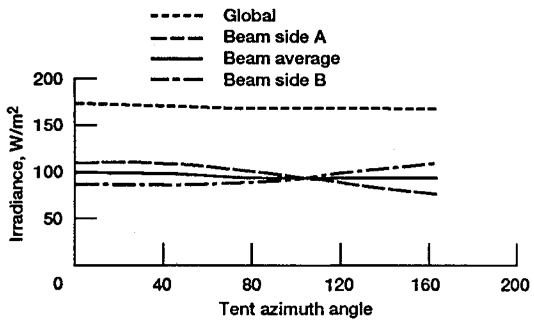

Fig. 4 Array specific mass variation with PV blanket end angle and area.

yearly average irradiance varies very little with tent orientation. However, the diurnal variation of the global irradiance, and hence, the time profile of the output power, changes significantly.[2] The azimuth angle for side A is measured from true S (0°) positively in a clockwise direction.

The solar cell efficiency values that were used in the analysis (given in Table 1b) are for 25°C and air mass zero. This was a conservative estimate since the operating temperature of the cells may be much lower, thereby increasing their efficiency.

Results

This analysis was performed to optimize a tent-shaped PV array for maximum specific power at the Viking landers locations (VL1: latitude 22.3°N, longitude 47.9°W, and VL2: latitude 47.7°N, longitude 225.7°W) on the Martian surface and with a variation in solar radiation corresponding to a full Martian year, a summer day and a winter day.

It has been shown in Ref. 10 that θ_l has no effect on the irradiance, and therefore, no effect on array output power. However, θ_l greatly affects the specific mass of the structure, Fig. 3. Therefore, the optimal shape of the blanket takes the natural catenary curve, i.e., $\theta_l = 0$ deg, which minimizes specific mass of the structure.

Structure specific mass (kg/m² of blanket) and array specific power (W/m²) are strong functions of the array tent angle θ_t. A typical effect of the tent angle on the specific mass is shown in Fig. 5 for carbon VHS composite, GaAs/Ge PV blanket, and wind speed of 20 m/s. This figure shows that the specific mass decreases with increasing tent angle, and the tendency is toward a bifacial vertical array. This is due to the fact that as θ_t approaches 90 deg, more of the loading is transmitted as compression in the vertical columns as opposed to bending, therefore, requiring less structural mass to support the array. The results for other material/PV blanket combinations were similar.

A stationary collector, either flat or curved (e.g., catenary), possesses an optimal inclination angle to maximize global irradiance, depending on the variation of the solar radiation throughout the year at the location latitude. The variation of the yearly average global irradiance as a function of θ_t is shown in Fig. 6. The optimal array tent angle is based on both the specific mass of the structure and the array output power, and is expressed by the specific power of the PV array in W/kg. This is shown in Fig. 7 for carbon VHS composite and GaAs/Ge at VL1 and for a wind speed of 20 m/s. Similar curves can be produced for all other structural material/PV blanket combinations.

With the optimal tent angle and blanket end angle for maximum specific power known, the remaining parameters D, W, and H can be determined. Since output power per area of PV blanket is independent of these parameters, they are determined by minimizing array structure mass per area of PV blanket. The procedure for this is given in Ref. 3, and the results are shown in Figs. 8, 9, and 10 for carbon VHS composite, GaAs/Ge blanket, 20 m/s wind speed, and θ_t =

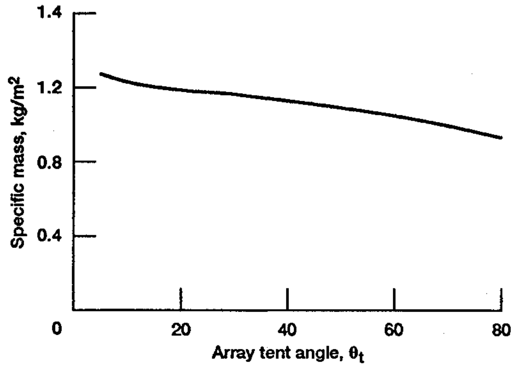

Fig. 5 Effect of the tent angle on the specific mass of the array (carbon VHS composite, GaAs/Ge solar cells, 20 m/s wind speed).

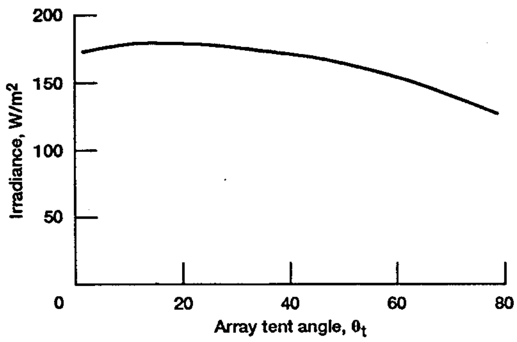

Fig. 6 Variation of the yearly average global irradiance as a function of tent angle.

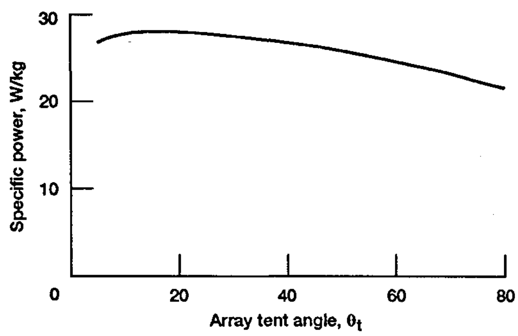

Fig. 7 Variation in specific power as a function of tent angle (carbon VHS composite, GaAs/Ge solar cells, 20 m/s wind speed at VL1).

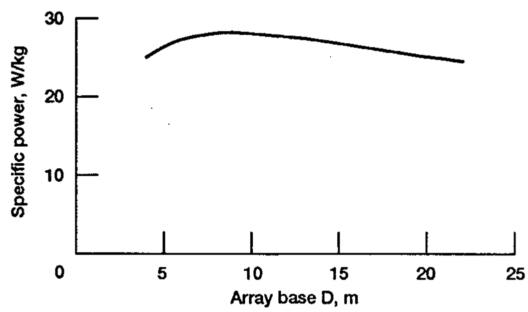

Fig. 8 Array specific power as a function of array D for W = 3.75 m (carbon VHS composite, GaAs/Ge solar cells, 20 m/s wind speed, 15-deg tent angle).

15 deg. Similar curves were produced for all structural material/PV blanket combinations. The results of the optimization process for the PV tent array are summarized in Tables 2 and 3.

The effect of season L_s and latitude ϕ on the PV array structure was also investigated. The solar irradiance of a sum-

Table 2 Performance results for various PV array/structural material combinations at the VL1 location based on yearly operation

	H, m	D, m	W, m	θ_t, deg	Blanket area, m^2	Total weight, kg	Specific mass, kg/m^2	Irradiance, W/m^2	Specific power, W/kg
Carbon VHS GaAs/Ge	1.16	8.69	3.75	15	34.16	40.97	1.1995	170.2	27.7
Carbon VHS silicon	1.39	8.56	3.75	18	34.30	33.29	0.9704	168.1	25.1
Carbon VHS GaAs CLEFT	1.47	8.51	3.75	19	34.35	30.89	0.8991	167.5	37.3
Carbon VHS amorphous Si	6.89	2.43	3.75	80	53.54	17.79	0.3323	113.1	34.0[a]
Aramid fiber GaAs/Ge	1.16	8.69	3.50	15	31.88	39.30	1.2330	170.2	26.9
Aramid fiber silicon	1.09	8.73	3.50	14	31.84	32.24	1.0123	170.6	24.4
Aramid fiber GaAs CLEFT	1.61	8.40	3.75	21	34.46	31.91	0.9270	166.5	35.9
Aramid fiber amorphous Si	6.89	2.43	3.75	80	53.54	18.40	0.3438	113.1	32.9[a]
Aluminum GaAs/Ge	1.97	4.53	3.25	41	20.54	30.72	1.4953	152.9	19.9
Aluminum silicon	2.12	4.24	3.25	45	20.66	25.46	1.2325	148.6	17.5
Aluminum GaAs CLEFT	2.72	4.41	3.25	51	24.12	26.90	1.1123	141.3	25.4
Aluminum amorphous Si	5.91	2.08	3.25	80	37.57	19.30	0.5138	113.1	22.0[a]
Magnesium GaAs/Ge	2.11	5.59	3.25	37	23.85	33.35	1.3985	155.5	21.7
Magnesium silicon	2.30	5.28	3.50	41	25.79	29.54	1.1454	152.9	19.3
Magnesium GaAs CLEFT	2.64	4.59	3.50	49	26.01	26.48	1.0181	143.3	28.1
Magnesium amorphous Si	4.92	1.74	3.50	80	35.08	15.57	0.4438	113.1	25.5[a]

[a]Not optimal solution.

Table 3 Effect of season and latitude on the array performance[a]

	L_s, deg	H, m	D, m	W, m	θ_t, deg	Blanket area, m^2	Total weight, kg	Specific mass, kg/m^2	Irradiance, W/m^2	Specific power, W/kg
VL1, ϕ = 22.3°	135	1.01	8.77	3.50	13	31.80	38.34	1.2058	289.8	46.9
	315	1.39	8.56	3.75	18	34.30	40.87	1.1916	147.9	24.2
	Year	1.16	8.69	3.75	15	34.16	40.97	1.1955	170.2	27.7
VL2, ϕ = 47.7°	135	1.01	8.77	3.50	13	31.80	38.34	1.2058	235.0	38.0
	315	1.39	8.56	3.75	18	34.30	40.87	1.1916	45.1	7.4
	Year	1.16	8.69	3.75	15	34.16	40.97	1.1955	152.9	24.9

Note: Carbon VHS, GaAs/Ge, 20 m/s wind speed.

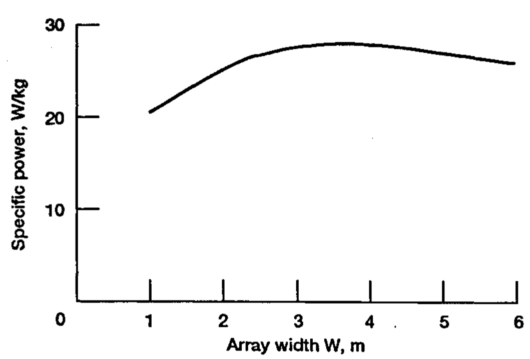

Fig. 9 Array specific power as a function array W for D = 8.69 m (carbon VHS composite, GaAs/Ge solar cells, 20 m/s wind speed, 15-deg tent angle).

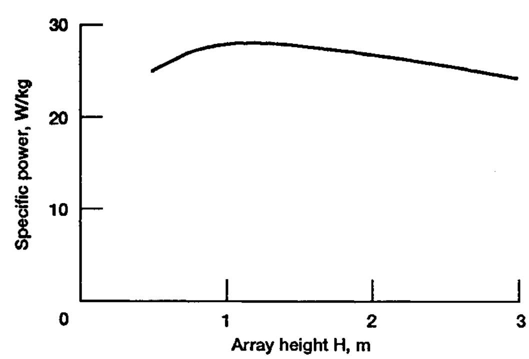

Fig. 10 Array specific power as a function of array H for W = 3.75 m (carbon VHS composite, GaAs/Ge solar cells, 20 m/s wind speed, 15-deg tent angle).

mer day L_s = 315° with an atmospheric opacity of 0.5, and a winter day L_s = 315° with an atmospheric opacity of 2.0, were compared with the yearly average irradiance for both Viking lander locations VL1 (ϕ = 22.3°) and VL2 (ϕ = 47.7°) as shown in Table 3. The results show that the latitude has no effect on the design point of the PV array. However, a higher specific power is obtained for the PV array at the lower latitude VL1 site due to higher irradiance. Higher specific power is obtained for a summer day than for a winter day. The optimum tent angle is lower for summer than for winter; and the yearly installation results in values between the summer and winter range.

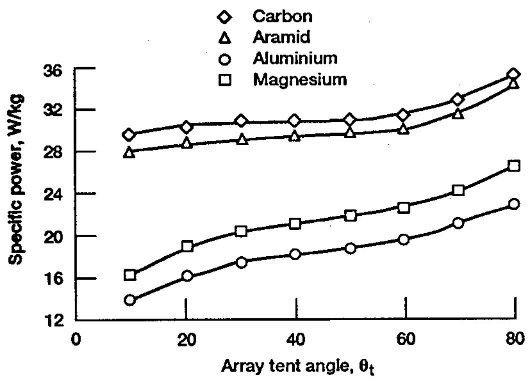

Fig. 11 Array specific power as a function of array tent angle for amorphous silicon blanket and different construction materials for W = 3.75 m, D = 8.69 m, 20 m/s wind speed.

The wind speed and the PV blanket cell efficiency have no effect on the optimal angle of the array.[1,3] By increasing the wind velocity, the required structural mass increases, and thereby increases the array specific mass.[3] This increase occurs uniformly for all structural materials and PV blanket types. The best combination of structure material and PV blanket remains the same. The PV blanket cell efficiency affects the array specific power but not the optimal design point.

Discussion

Through the analysis it was determined that, of all the structural material/PV blanket combinations, the highest specific power (37.3 W/kg) is obtained using carbon VHS composite structural material and a GaAs CLEFT PV blanket. The results for the amorphous silicon are marked with an asterisk, which require an explanation. The optimal solution for this combination is obtained for $\theta_t \approx 90$ deg (i.e., a vertical surface with solar cells on both sides). The reason for it resides in the fact that amorphous silicon has a much lower blanket specific mass than the other types of PV blankets. As a result, the specific mass of the structural material decreases much more rapidly with increasing θ_t than it does with the other PV blankets. The values in Table 2 for amorphous silicon are calculated for θ_t = 80 deg. Figure 11 shows the variation of the specific power with tent angle for the four types of structural materials with an amorphous silicon blanket.

In a situation where the array design must be altered or where one or more of the geometry variables are constrained, e.g., the catenary blanket being annexed to an existing structure, a new optimization would have to be performed based on the remaining unrestricted variables. It should be mentioned that not all PV blankets have the same design. This aspect was not discussed in this study.

The effect of self-shadowing of a catenary-tent-PV array on its power output was also not addressed in the present article. Shadow patterns, however, are discussed in Ref. 10.

The low operating temperature of the solar cells on Mars will increase the cell conversion efficiency by a greater amount for cells with higher temperature coefficient, and thus reduce the advantage in the cell efficiency of GaAs solar cells over silicon. The sunlight on Mars is also spectrally shifted (reddened) due to dust. The peak of the atmospheric transmission of Mars is about 0.8 μm. This peak is close to the peak spectral response wavelength of both silicon and GaAs cells that may result in a slight increase in the conversion efficiency. These issues were not, again, addressed in the present study.

Conclusions

To provide electrical power during an exploration mission to Mars, a deployable tent-shaped structure having a flexible catenary photovoltaic blanket is analyzed. The PV blanket shape and the array dimensions were optimized to achieve a configuration that maximizes the specific power (W/kg) of the array. The natural catenary shape of the PV blanket, i.e., θ_1 = 0 deg, was determined by the array specific mass. θ_t was determined by the combined effect of structural specific mass and PV array output power. This angle varied for different structural material/PV blanket combinations. The combination of carbon VHS composite structural material and GaAs CLEFT solar cells produces the highest specific power. A high specific power is also obtained with an amorphous silicon PV blanket as the tent approaches a vertical shape. The study refers to two locations on Mars, VL1 and VL2. The latitude of the location has no effect on the design point of the PV array, at least for the examined sites. Lower tent angles were obtained for summer operation, then for winter. The tent azimuth has almost no effect on the optimal design point. The wind speed and PV blanket cell efficiency affects the numerical value of array specific power, but not the optimal design point.

Acknowledgment

This work was funded under NASA Grant NAGW 2022.

References

[1]Landis, G. A., Bailey, S. G., Brinker, D. J., and Flood, D. J., "Photovoltaic Power for a Lunar Base," *Acta Astronautica*, Vol. 22, 1990, pp. 197–203.

[2]Hickman, J. M., Landis, G. A., and Curtis, H., "Design Consideration for Lunar Base PV Power Systems," *Proceedings of the 21st IEEE Photovoltaic Specialists Conference* (Orlando, FL), Vol. 2, 1990, pp. 1256–1262.

[3]Colozza, A. J., "Design Optimization and Analysis of a Self-Deploying PV Tent Array," NASA CR-187119, June 1991.

[4]McCormick Barnes, W., *Aerodynamics, Aeronautics, and Flight Mechanics*, Wiley, New York, 1979.

[5]Gaier, J. R., Perez-Davis, M. E., and Marabito, M., "Aeolian Removal of Dust from Photovoltaic Surfaces on Mars," NASA TM-102507, Feb. 1990.

[6]Lovell, D. R., "Carbon Fiber Composite Reciprocating Guide Bar," *Carbon Fibers, Technology, Uses and Prospects*, Plastic and Rubber Inst., London, 1986, pp. 176–182.

[7]Beer, F. P., and Johnston, E. R., Jr., *Mechanics of Materials*, McGraw-Hill, New York, 1981.

[8]Piszczor, M., "Specifications of Various PV Blankets," Photovoltaic Branch, NASA Lewis Research Center, Internal Rept., Cleveland, OH, June 1990.

[9]Hanak, J. J., Fulton, C., Myatt, A., Nath, P., and Woodyard, J. R., "Ultra-Light Amorphous Silicon Alloy Photovoltaic Modules for Space and Terrestrial Applications," *Proceedings of the 21st IEEE Intersociety Energy Conversion Engineering Conference*, Vol. 3, 1986, pp. 1436–1440.

[10]Crutchik, M., and Appelbaum, J., "Solar Radiation on a Catenary Collector," *Space Power*, Vol. 11, Nos. 3 and 4, 1992, pp. 215–240.

[11]Appelbaum, J., Landis, G. A., and Sherman, I., "Solar Radiation on Mars—Update 1991," *Solar Energy*, Vol. 50, No. 1, 1993, pp. 35–51.